Light Metals 2015
Edited by: Margaret Hyland
TMS (The Minerals, Metals & Materials Society), 2015

EFFECT OF ELECTROMAGNETIC FIELDS ON THE PRIMING OF HIGH GRADE CERAMIC FOAM FILTERS (CFF) WITH LIQUID ALUMINUM

Robert Fritzsch[1], Mark William Kennedy[1,2], Shahin Akbarnejad[3], Ragnhild E. Aune[1]

[1]Dept. of Materials Science and Engineering, Norwegian University of Science and Technology (NTNU), Trondheim, NORWAY
[2]Proval Partners S.A., 70 Rue de Genève, 1004 Lausanne, SWITZERLAND
[3]Department of Materials Science and Engineering, Royal Institute of Technology, 100 44 Stockholm, SWEDEN.

Communicating author: robert.fritzsch@ntnu.no

KEYWORDS: Electromagnetism, Priming, Aluminum, CFF, Liquid Metal, Filtration

Abstract

Electromagnetic fields can influence the behavior of liquid metals in commercial Ceramic Foam Filters (CFF's). In the present study 9 inch industrial CFF's of high grade with 50 and 80 pores per inch (ppi) have been investigated. The main objective was to prime the 9 inch industrial scale CFF's with a standard aluminum casting alloy (3XXX - alloy) by the use of various magnetic field strengths (max. 0.12 T) induced by a coil. The obtained results were compared with reference gravity experiments. The influence of the electromagnetic Lorentz forces on the obtained results was calculated with 2D Finite Element Modeling (FEM) using the COMSOL® software. The fluid flow characteristics inside the CFF were considered and are part of another publication within the group.

Introduction

Aluminum melts contains a large number of inclusion particulates of ≤ 50 µm in size. These inclusions may be particles, bifilms or clusters of: oxides (Al_2O_3, SiO_2), spinels ($MgO{\cdot}Al_2O_3$), carbides (SiC, Al_4C_3), nitrides (AlN), borides (TiB_2), sulfides, phosphides and intermetallics [1]. Large concentrations or inclusions over a critical size limit can render the metal un-fit for industrial applications and result in serious financial consequences for metal producers. Many types of inclusions in the aluminum melt can have a negative impact on the machinability, mechanical properties, and can lead to increased gas porosity and shrinkage of the metal during casting [1]. Use of more post-consumed and process aluminum scrap further increases the potential for melt contamination by inclusions. This results in greater challenges to achieve metal yield and the required quality standards. These challenges can be expected to increase in the future.

In recent years, the aluminum industry has developed a number of treatment processes to improve metal cleanliness. CFF's are the most commonly applied filtration technology for aluminum alloys and have been used to filter over 50% of the world production of aluminum since the 1990's [2].

Electromagnetically (EM) enhanced filtration of aluminum has been the topic of recent studies [3]. Batch experiments with filters and liquid metal have been conducted to understand the impact of the magnetic field on the metal flow and particle migration inside the filter [4]. Flow filtration experiments with an applied EM field using a small scale setup, have been executed to investigate the effect also on the filtration efficiency [5]. All experiments that have been conducted so far were using 30, 50 and 80 ppi CFF's and using A356 aluminum alloy.

In the course of the previous filtration work it was discovered that priming of the filters, defined as the filling of the pores with metal and the removal of entrained gas, could also be achieved using the EM Lorentz forces produced in liquid metal by the alternating current induction coil. It was found that the Lorentz forces could be used to prime CFF's of up to 80 ppi without preheating and using only a fraction of the metal head that was typically required in conventional industrial filter units. These studies applied 100 to 150 mm of metal head to prime CFF's with an 80 ppi grade [4, 5] instead of the typical industrial values of up to 350 mm, showing that it was primarily the EM forces and not gravity, which primed the filters. The discovery of electromagnetic priming is now the subject of a US patent application [6].

Recently, the effect of an electromagnetic field generated by a square helically wound induction coil on the priming of a 9 inch commercial CFF has been the subject of experimental study. The current study focuses on the design and verification of a pilot scale filter unit, including the induction coil and the filter box. The required metal head to sufficiently prime and wet a commercial 9 inch filter with liquid aluminum is the main topic of this article. Experimental and FEM results computed using the multi-physics software COMSOL® will be presented.

Theory

In a helically wound induction coil an applied alternating current flows primarily in the phi direction and generates a time varying magnetic flux density $B_z\ [T]$ in the z-direction of the coil (noting that strong radial components also exist in the flux at the ends of the coil). The z-component of the magnetic flux then induces a current $J_\phi\ [A/m^2]$ that opposes the main current in accordance with Lenz's law and the conservation of energy, in this case in the negative phi direction.

It is known that 'short' induction coils have a gradient in the local flux density B_z along the z-axis. The gradient in the magnetic field results in a similar variation in the magnitude of the induced current in the liquid metal. The magnitudes of the induced current are furthermore influenced by the effective electrical conductivity within the filter media. The current and the magnetic flux therefore have different magnitudes above, within and under the filter. For a given applied current, filter type and aluminum conductivity the position of the filter within the coil then determines the amount of current induced by the local magnitude of the EM field.

Lorentz forces F_L $[N/m^3]$ are the cross product of the induced current density and the magnetic flux, as shown by [Eq. 1]. These forces act axial symmetrically on the aluminum and ignoring the small radial component of the flux density, can be assumed to act exclusively in the r-direction.

$$F_L = J_\phi \times B_z \qquad \text{[Eq. 1]}$$

The coil was placed as shown in Figure 1 in order to maximize both the magnitude of the EM field on the surface of the filter and the curl in the induced Lorentz forces. Prior to priming, there is no electrical conductivity in the CFF and therefore no induced Lorentz forces. Therefore there initially exists a very strong axial gradient of F_L in the z-direction, which results in forceful Magneto-Hydro-Dynamic (MHD) movement and hence, the initial priming of the filter.

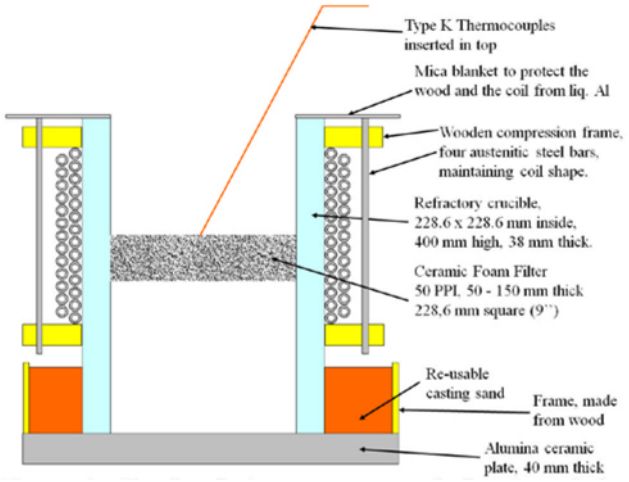

Figure 1: Sketch of the apparatus used for the priming experiments. The coil is placed with its center line at the top line of the CFF to generate the highest flux density at the entrance to the filter. During the experiments the coil was compressed by a wooden frame, covered in alumina sheets, to suppress vibrations and protect it from mechanical and thermal damage.

The difference in the effective conductivity of the filter area and the liquid metal region ensures a continuing curl in the Lorentz forces and continuing strong MHD mixing even after the initial priming [4]. This continuing MHD mixing also ensures that gas bubbles are removed and wetting is improved within the CFF after some time. The time varying value of the Lorentz forces induces metal vibrations, which combined with inductive heating, may contribute to improved gas release and wetting of the CFF by the liquid metal.

The effective conductivity of the filter region is determined by the porosity and tortuosity of the ceramic material. The effective conductivity was directly measured using reference metal of a known conductivity in a special coil set-up completely filled with liquid metal impregnated CFF's. The effective electrical conductivity could then be determined by the reduction in the induced power from the metal-only case. Estimates of tortuosity were then made from the effective electrical conductivity and the measured total porosity [7].

$$\frac{\sigma_m}{\sigma_f} = \frac{\tau}{\varepsilon} \qquad \text{[Eq.2]}$$

Where σ_f is the effective electrical conductivity of the filter media [S/m], σ_m is the conductivity of the metal [S/m], τ is the tortuosity [unit less] and ε as the total porosity [%].

The effective conductivity is essential to be able to generate 2D axial symmetric multi-physics models. The validation of the COMSOL® models for heating and for the magnetic field has been published elsewhere [8-10]. The method was successfully applied to round 100 mm filters in flow and batch experiments [11] and is now being applied on this next step to large industrial scale, i.e. the 9" or 229 mm scale.

Experimental Method and Materials

A square induction coil was built to generate an EM field, induce current and Lorentz forces in liquid aluminum within a standard commercial 9 inch filter. A schematic of the experimental setup used is shown in Figure 1. The experimental setup was designed to generate strong axial magnetic fields in the area of the CFF. Strong 100 Hz electro-mechanical vibrations were induced by the low frequency alternating current and this required powerful restraints to hold the coil as indicated in the photograph shown in Figure 2.

Batch filtration experiments were conducted using ~8 kg of molten aluminum with the composition given in Table 1. The melt for the experiments was prepared in a standard resistance furnace with a holding temperature of 800°C. After skimming of the dross the metal was manually poured on the CFF. No pre-heating was applied; the filter was at room temperature prior to pouring. The temperature of the metal before casting was measured to be ~760°C. To prove that the filters do not prime by gravity forces the metal rested for a time of 15s above the filter before the current was applied to the coil. Pure gravity reference experiments have been conducted earlier [4], which validated the negligible penetration of liquid metal into the filters without sufficient metal head (100 mm was used).

The EM experiment was initialized by energizing the double coil at 50 Hz with 1250 A ±1% and 1 A resolution (RMS), generating a magnetic field strength of ~0.12 T ±1% at the center line of the empty coil as measured using a Hall Effect gauss meter model 6010 engineered by Pacific Scientific OECO, F.W. Bell®. The axial probe was standardized using an axial standard of 0.05 T ± 0.3 mT. The magnitude of the magnetic field was then compared by measuring the applied AC current

and the induced power using a Fluke® 43B Power Quality Analyzer with a resolution of 100 W. The current was measured by a inductive current probe i1000S with a resolution of 1 A and ±1%, engineered by Fluke®. The conductivity at room temperature of the used metal was determined by an AutoSigma 3000 electrical conductivity meter with an accuracy of ±0.5% using a high frequency probe. The resulting numbers were used to calculate valid FEM simulation results, i.e. no fitting parameters of any kind were used during the simulations.

Initial priming occurred 6 to 10 seconds after the field was activated and it was turned off after the priming was finished, i.e. when the metal reservoir above the filter was fully drained. The metal remained in the crucible to cool down and solidify. After solidification, the filter has been sectioned to investigate the wetting behavior and the remaining gas inside the filter.

Table 1: The chemical composition in wt. [%] of the aluminum alloy.

Alloy	Si	Fe	Cu	Mn	Zn	Al
3xxx	0.06 – 0.12	0.17 – 0.22	0.1 – 0.15	0.95 – 1.05	0.15 – 0.2	remaining

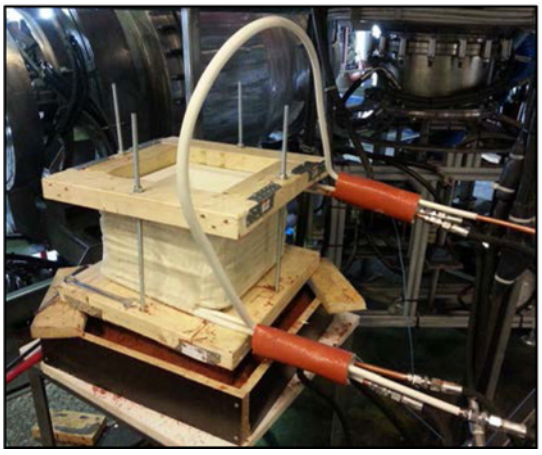

Figure 2: Experimental apparatus for the 9 inch filter experiment, showing the uncompressed double coil (and large loop 'jumper') made of 12 mm copper tubes, the wooden frame to suppress vibrations, the refractory crucible, embedded into red casting sand, and the high pressure hose system for cooling.

Priming and Wetting Results and Discussion

CFF's applied in industry are normally operated in a filter box, which uses a certain gravity head of liquid metal and a recommended pre-heating technique to achieve priming [12]. Gravity forces the metal into and through the filter, removing a sufficient fraction of the interstitial air and partially wetting the filter media. In Figure 3 typical magnitudes of industrial priming heights are shown [11, 13, 14].

The impact of EM enhanced priming was very significant in earlier experiments and further increased in the current investigation. The experimental trial to investigate lower metallostatic pressure involved priming a 50 ppi CFF with a target of 50 mm metal head (56 mm was actually applied). The head proved to be sufficient to prime the filter without freezing or blocking of the CFF as indicated in Figure 3.

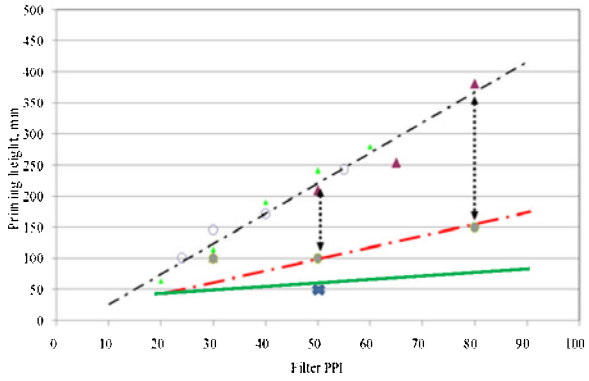

Figure 3: Priming height vs. filter ppi from different producers [13, 14] compared to the earlier conducted electromagnetic priming at 0.17 T using 100mm round CFF (red dotted line) [11] and the new results using 0.12 T on a 9'' filter (full line and cross).

In Figure 4 a) to d), the results of the successful low metal head experiment are shown. 56 mm metal head generated by ~8 kg of liquid aluminum were poured on an un-preheated 50 ppi CFF and were allowed to rest for 15 seconds on the filter without any field or stirring, as shown in Figure 4 a). In Figure 4 b) the coil was electrified with 1250 A (RMS) generating a magnetic field that formed a stable meniscus as shown in Figure 6 c). The filter started to prime after 6 seconds finished after 10 seconds as shown in Figure 4 d).

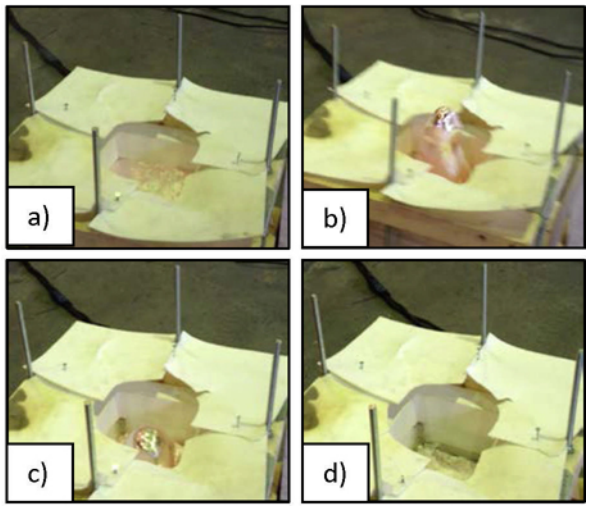

Figure 4: Trial of a low metal head priming experiment, using 56 mm of height above the 9'' 50 ppi CFF. Image a) shows the metal resting above the filter for 15 seconds without any effect (casting temperature ~760°C). Image b) shows the effect of the electromagnetic field when activated with full strength of 0.12 T. Image c) shows that the metal then formed a stable meniscus and it took in total 6 seconds to begin to prime the metal through the CFF, as show image d).

Due to the low metal head and the position of the filter within the coil, a strong and stable meniscus with the height of approximately 160 mm was formed by the interaction of the EM Lorentz forces, surface tension and gravity. The creation of a meniscus would logically appear to be highly beneficial to improving the priming of a filter by using the EM forces to artificially increase the effective gravity forces. Therefore the effective metal head in the center of the meniscus was approx. 160 mm, which is still not sufficient to prime the 50 ppi CFF by gravity force alone as indicated by the industrial data for pre-heated filters shown in Figure 3. Figure 5 shows a 'steady state' FEM solution of the flow field of the metal inside the meniscus. It shows a strong push into the filter in the center of the meniscus in addition to the 'enhanced' gravity force. This may be the reason that priming was effective with such a low initial metal height of 56 mm. The interaction of gravity and Lorentz forces generate strong flow patterns, which further aid the priming. This was discovered and investigated by the research group earlier [15].

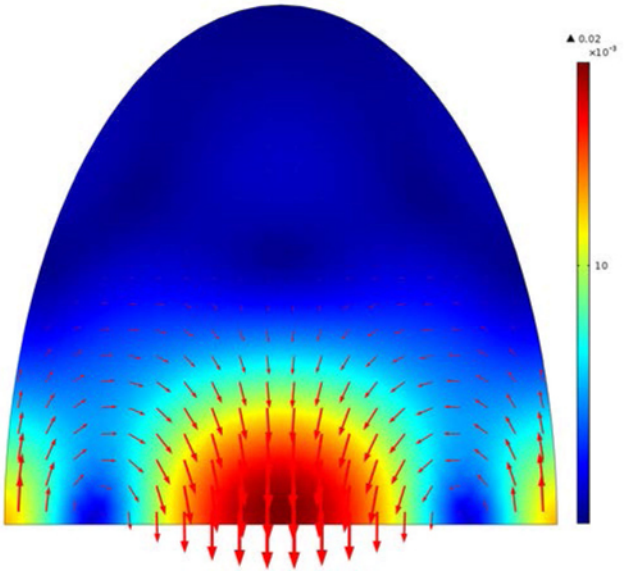

Figure 5: Steady state FEM model generated with COMSOL® 4.4 shows the induced flow field during the priming stage inside the meniscus. The bottom line represents the filter surface and is modeled as an open border boundary condition. The driving force of gravity and of the flow field into the filter is highest at the center.

Higher grade CFFs, such as: 50, 60 or even 80 ppi; have a higher tortuosity and less web-like structure than low grade: 30 and 20 ppi which are more commonly applied. The longer path length and more labyrinth-like structure favors the trapping of air inside the filter, the creation of dead zones and the freezing of metal during the priming stage. Freezing would result in a blockage of the filter prior to priming. The good mixing and inductive heating, together with the strong electromagnetic 'push' into the filter reduces the chance of freezing filters prior to priming.

An experimentally validated FE-model for a meniscus can be seen in Figure 6 [16]. This model shows a meniscus with a solid plate at the bottom. The induced current generates strong MHD-mixing and the flow field results in a stable meniscus. The metal homogenizes inside the meniscus, generates a flow field in a shape of a loop as seen in Figure 6 and eventually melts any frozen metal at the surface of the filter, such that the metal gets pushed into the filter as indicated in Figure 5.

The total area available for particle attachment of each CFF varies by the differences of wetted surface, dead volume and entrapped air. In the literature the total filtration efficiency varies in some cases up to 70% [12]. It is expected that a fully wetted filter has a larger surface area for filtration and lower pressure drop during the filtration. Some of the variation of filtration efficiency might be correlated with insufficient filter priming, a large variation of the internal area available for flow and resulting changes in the so called 'interstitial' velocity due to partial blockage by air.

The less volume that is available for fluid flow, the higher the resulting interstitial velocity inside the filter channels and therefore, the lower the resulting filtration efficiency of the filter in accordance with the models of Apelian [17], shown with [Eq.3]. Increasing the amount of fully wetted filter surface could therefore increase the overall filtration efficiency as proposed earlier [11]. Reducing the pressure drop of the filter and allowing thicker filters to be applied will make it easier to adjust the filter throughput to the required metal cleanliness. The correlation is shown:

$$E_0 = 1 - exp^{-\frac{K_0 L}{u_s}} \qquad \text{[Eq.3]}$$

Where E_0 is the filtration efficiency, K_0 is the kinetic parameter [1/s], defined by Apelian, L as the physical thickness of the filter [m] and the superficial velocity u_s in [m/s].

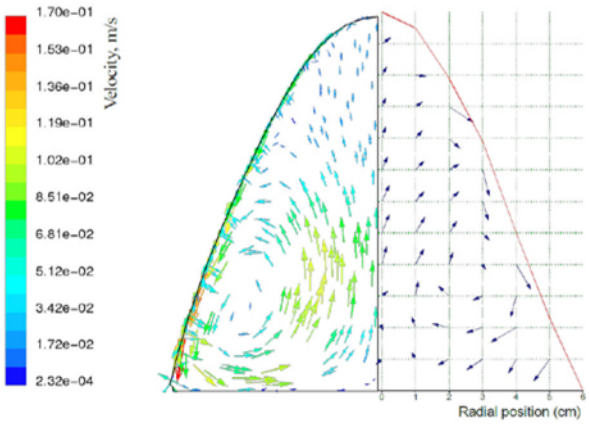

Figure 6: Visualization of a k-ε turbulence model showing a sodium meniscus. Left is the model and right is the measured velocity **[16].**

Metallostatic Pressure and required Metal Head

The required pressure to prime is traditionally created by the metal head above the filter. After the priming the metal head also creates the pressure to sustain the desired superficial velocity. To estimate the required metal head for either of the steps, the knowledge of the tortuosity and porosity of each filter type is essential. The tortuosity is necessary to calculate the interstitial velocity, which represents the real velocity inside the

filter media and can be calculated as shown in [Eq.4]. Due to the reduced area inside the filter for the flow and the incompressible liquid the interstitial velocity will be greater than the superficial velocity. The interstitial velocity has a major effect on the filtration efficiency; making filtration modes such as sedimentation by gravity inside the filter less favored in higher ppi CFF's. Theoretical calculations on the filtration modes related to the interstitial velocity have been presented elsewhere [5].

$$v_i = \frac{v_s \tau}{\varepsilon(1-f_d)} \qquad \text{[Eq.4]}$$

Where v_i is the interstitial velocity [m/s], τ is the tortuosity [unitless], ε is the total porosity [unitless] and f_d is the fraction dead volume [unitless] of the total filter volume.

The dead volume is estimated to be of the order of 30%, as results in the literature vary between 16 to 40% [5, 18, 19]. Using this dead volume and the porosities and tortuosities as shown in Table 2, results in an increase of the effective velocity inside the filter (v_i/v_s) by a factor of 2.1 for a 30 ppi, 3.6 for a 50 ppi and 5.3 for an 80 ppi CFF.

The resulting interstitial velocity has a critical impact on the probability of particle collection. Filtration mechanisms have been discussed in earlier publications [3, 5], showing settling and bridging (cake filtration) as the main filtration modes. Both mechanisms suffer at higher interstitial velocities, resulting in the need for larger or thicker filters. Higher interstitial velocity would increase the effect of inertia, direct interception and effects of turbulence [20]. Filtration mechanisms and efficiencies have not been a topic in this investigation and are part of the plans for future work.

Flow through a porous media as defined by the superficial velocity creates a pressure gradient, which can be calculated using the Forchheimer equation [Eq.5].

$$\Delta P = L\left(\frac{\mu}{k_1} v_s + \frac{\rho}{k_2} v_s^2\right) \qquad \text{[Eq.5]}$$

Where ΔP is the pressure drop [Pa], L is the thickness of the filter [m], μ is the dynamic viscosity [Pa*s], v_s is the superficial velocity [m/s], ρ is the fluid density [kg/m^3], k_1 [m^2] and k_2 [m] are empirical permeability constants. The recommended values for the Darcian and non-Darcian terms k_1 and k_2 are topic of another publication [21] and have been compared with earlier publications [5, 11].

The pressure drop is not dependent on the size or shape of the filter, but on the thickness and the resistance of the filter to flow. Therefore pressure drop is strongly influenced by the filter grade or ppi, as represented by the permeability constants which define the resistance of the filter to flow. The required metal head for the priming and to maintain a given superficial velocity during filtration is therefore highly dependent on the thickness and type of the filters. The dead volume, tortuosity, and porosity of the filter relate strongly to the permeability constants and hence the total pressure drop for a given metal flow rate per unit filter area.

CFF's are typically 50 mm thick plates which are relatively difficult to efficiently prime. Problems in priming have been a barrier to the use of increased thickness to achieve higher filtration efficiencies. The technology to sufficiently prime various thicknesses of high ppi CFF has been recently patented [6] and further steps are initiated.

The graph in Figure 7 shows the required metal head after priming to maintain a superficial velocity (i.e. casting rate) using 50 and 150 mm filter thicknesses, for 30 (solid line) and 80 (dashed line) ppi CFF. A thicker filter will have a substantially increased filtration efficiency as indicated by equation 3 by Apelian [17]. The analytical solution reveals that the required metal head for a fully primed 150 mm thick 80 ppi CFF will be 100 mm to maintain 9 mm/s superficial velocity through the filter, which is a standard casting velocity for billet casing in industry as shown in Table 2. An inefficiently primed filter will have blocked areas (retained gas) and areas of higher and lower interstitial velocity. Overall the filter will have both higher pressure drop and lower filtration efficiency.

Table 2: Data used for simulation and calculations regarding the used CFF. [3]

Grade [ppi]	Porosity [%]	Tortuosity, τ	Darcy Constant k_1 [m^2]	Forchheimer 2nd Order k_2 [m]
30	0.892	1.3	5.08E-08	5.46E-04
50	0.863	2.2	1.57E-08	1.66E-04
80	0.865	3.2	6.52E-09	1.15E-04

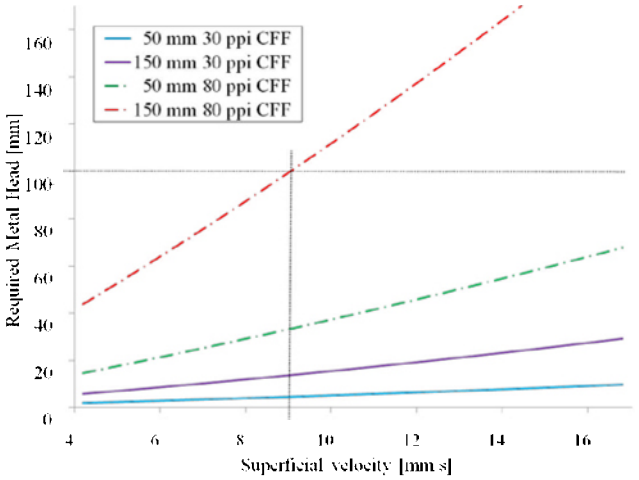

Figure 7: Calculated metal head to maintain a given filtration superficial velocity in mm/s through the filter. As an example, the dark lines indicate that at 100 mm of head for EM priming, a gravity flow of 9 mm/s, which is typical of an industrial billet casting velocity, can be maintained for a 150 mm thick high grade 80 ppi CFF.

Multi-Physics Modelling

To develop a better understanding of the influence of the EM field on the behavior of the liquid metal entering and flowing through the filter, 2D axial symmetric FE modeling using COMSOL® 4.4 was used to solve for the steady state Lorentz force and flow fields. The EM field for the priming case is shown in Figure 8.

It has been shown in previous research that sufficient head over the coil can suppress the formation of a meniscus. The following CFD models therefore assume no meniscus in contrast to the experiment modelled in Figure 5. The simulation starts with no metal inside the filter and therefore no Lorentz forces are induced inside or below the CFF. The metal above the filter will experience powerful induced Lorentz forces, as shown in Figures 8 and 9 for a 228 mm filter. Combined with the lack of Lorentz forces in the un-primed filter region it results in a strong MHD flow pushing the metal into the filter as shown in Figure 9. The velocity field shown in Figure 9 is at the exact moment priming is initiated.

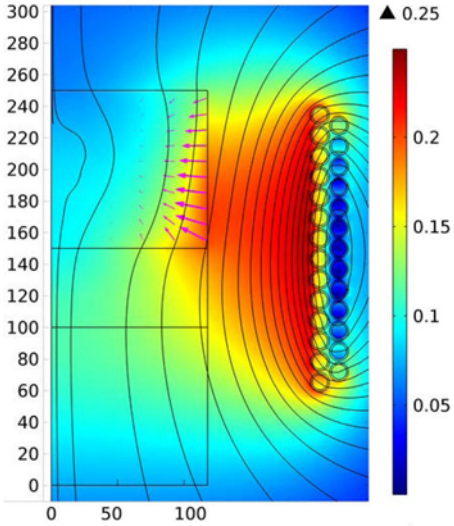

Figure 8: Steady state axial symmetric COMSOL® model of the experimental setup during priming (no metal in or under the CFF). The axis of symmetry is located at r = 0, the coil to the right, the highest square represents the metal above the filter before priming. The stream lines and the surface show the magnetic flux density (normalized in [T]) and the magenta colored arrows show the time averaged Lorentz force contribution (F_L) inside the liquid metal.

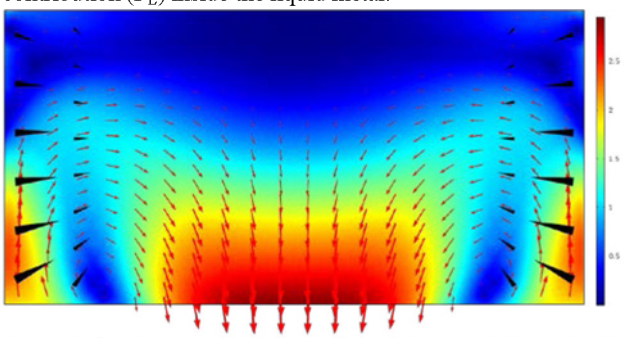

Figure 9: Steady state CFD simulation of the metal above the 9'' CFF showing the initial induced flow field during the start of priming. The colors imply that the application of 1250 A(RMS) current induce a superficial velocity of 2.5 m/s in the center of the filter. The resistance of the filter to priming can generate a meniscus above the filter as shown in Figure 4 b) and c) and Figure 5 until the resistance/blockage of the filter is broken (re-melting the metal that blocks the cold filter) and the metal penetrates into the filter. Sufficient height of metal over the coil can suppress meniscus formation.

After the filter and the volume below are filled with metal, the velocity field changes direction and generates a strong back mixing effect, discussed in earlier publications [4, 5, 15]. The magneto hydrodynamic (MHD) mixing for the filled crucible, coil position and RMS-magnitude of Lorentz forces (black cones) is shown in Figure 9. The simulation uses the properties of a 50 ppi CFF, as presented in Table 2.

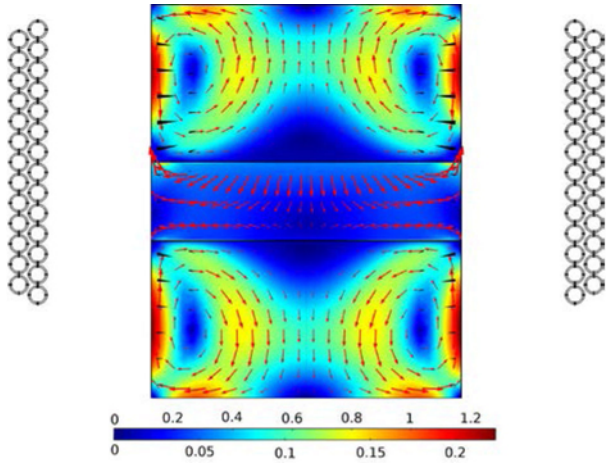

Figure 10: Flow field simulation showing the MHD for a 9" 50 ppi CFF using a 27 turn double coil with an applied alternating current of 1250 A (RMS). The coil position is centered at the upper line of the filter to guarantee a maximal force during the priming stage. Peak velocities are calculated to be 1.28 m/s in the metal and 0.22 m/s in the filter. The top legend is scaled for the metal region, and at bottom for the filter region, both in m/s. The red arrows indicate the direction and magnitude of fluid flow and the black cones the Lorentz forces in metal and porous media regions; sizes are not comparable between regions.

The air gap results in a significant reduction in magnetic field and induced Lorentz forces in the liquid metal. Application of 1250 A (RMS) generates a sufficiently strong EM field to prime the filters and inducing a velocity of up to 0.22 m/s inside the filter and more than 1 m/s in the metal phase after priming.

Conclusions

The effect of an electromagnetic field on the priming of a small 9" commercial Ceramic Foam Filter (CFF) has been demonstrated with less metal head than anticipated based on previous experiments [11] and much less than standard industrial priming heads [13, 14]. Priming of a 50 ppi CFF succeeded with only 56 mm metal head, which is less than 25% of the standard metal head used by industry today. Electromagnetically enhanced priming will enable higher grade (higher ppi) or thicker CFFs to be used with standard priming heights.

Increasing the available area for filtration by greater removal of gas from the inside of the filters, as well as improved filter wetting will allow higher throughput and casting velocities while not altering the filtration efficiency of the applied filter grade. This might allow an optimized (similar) metal head for both priming and casting, implying the use of thicker filters.

An improved the melt quality can be achieved by removing more solid inclusions using a higher grade filter, a thicker filter or slower filtration. With EM priming a higher grade and/or thicker filter can both be primed efficiently with low metal head achieving higher filtration efficiencies for a given filter box installation.

Future Work

Priming trials will be executed using the 9'' industrial size filter box with 30 to 80 ppi CFFs. A stack of up to three 50 mm thick commercial filters will be used. Flow experiments with artificial inclusions will be used to investigate filtration efficiency and the behavior of stacked filters in order to verify the casting rate estimates shown in Figure 7.

Metallographic investigations will be carried out on particle distribution, and to study the filtration mechanisms and interfacial wetting between alumina and aluminum.

Acknowledgements

The industrial partners involved in the project are: Hydro Aluminium AS supporting with casting alloys, Norwegian University of Science and Technology (NTNU) and SINTEF Materials and Chemistry.

The authors also wish to express their gratitude to Kurt Sandaunet and Roar Jensen from SINTEF and Trygve Schaunche from NTNU for their support and help, as well as for the use of the casting laboratory of the Institute for Material Technology (IMT) at NTNU, Trondheim in Norway.

Reference

1. D. E. Groteke, "The Reduction of Inclusions in Aluminum by Filtration," Modern Casting, vol. 73, 1983, pp. 25-27.
2. K. Butcher and D. Rogers, "Update on the filtration of aluminum alloys with fine pore ceramic foam," 1990, pp. 797-803.
3. M. W. Kennedy, "Removal of Inclusions from liquid Aluminium using Electromagnetically Modified Filtration," PhD, Department ofMaterials Science and Engineering, NTNU, Trondheim, 2013.
4. R. Fritzsch, M. W. Kennedy, S. Akhtar, J. A. Bakken, and R. E. Aune, "Electromagnetically Modified Filtration of Liquid Aluminium with a Ceramic Foam Filter," Electromagnetic Processing of Materials (EPM2012), Beijing, China, 2012.
5. M. Kennedy, R. Fritzsch, S. Akhtar, J. Bakken, and R. Aune, "Electromagnetically Modified Filtration of Aluminum Melts Part II: Filtration Theory and Experimental Filtration Efficiency with and without Electromagnetic Priming for 30, 50 and 80 PPI Ceramic Foam Filters," To be submitted to Metallurgical Transactions B, 2012, pp. 1-69.
6. M. W. Kennedy, R. Fritzsch, S. Akhtar, J. A. Bakken, and R. E. Aune, "Apparatus and Method for Priming a Molten Metal Filter," U.S. Patent, 2012.
7. M. W. Kennedy, K. Zhang, R. Fritzsch, S. Akhtar, J. A. Bakken, and R. E. Aune, "Characterization of ceramic foam filters used for liquid metal filtration," Metallurgical and Materials Transactions B, vol. 44, 2013, pp. 671-690.
8. M. W. Kennedy, S. Akhtar, J. A. Bakken, and R. E. Aune, "Analytical and Experimental Validation of Electromagnetic Simulations Using COMSOL®, re Inductance, Induction Heating and Magnetic Fields," COMSOL Users Conference, Stuttgart Germany, 2011.
9. M. W. Kennedy, S. Akhtar, J. A. Bakken, and R. E. Aune, "Analytical and FEM Modeling of Aluminum Billet Induction Heating with Experimental Verification," TMS Light Metals, Orlando Florida, 2012.
10. M. W. Kennedy, S. Akhtar, J. A. Bakken, and R. E. Aune, "Improved Short Coil Correction Factor for Induction Heating of Billets," EPD Congress, Orlando Florida, 2012.
11. R. Fritzsch, M. W. Kennedy, J. A. Bakken, and R. E. Aune, "Electromagnetic Priming of Ceramic Foam Filters (CFF) for Liquid Aluminum Filtration," TMS Light Metals, 2013, pp. 973-979.
12. S. Ray, B. Milligan, and N. Keegan, "Measurement of Filtration Performance, Filtration Theory and Practical Applications of Ceramic Foam Filters," 2005, pp. 1-12.
13. J. E. Dore and C. Bickert, "A Practical Guide on How to Optimize Ceramic Foam Filter Performance," Light Metals, 1990, pp. 791-796.
14. N. Keegan, W. Schneider, and H. P. Krug, "Evaluation of the efficiency of fine pore ceramic foam filters," Light Metals-Warrendale, 1999, pp. 1-1.
15. M. W. Kennedy, S. Akhtar, J. A. Bakken, and R. E. Aune, "Electromagnetically Enhanced Filtration of Aluminum Melts," TMS Light Metals, 2011 pp. 763-768.
16. E. Baake, A. Umbrashko, B. Nacke, A. Jakovics, and A. Bojarevics, "Experimental investigations and LES modelling of the turbulent melt flow and temperature distribution in the cold crucible induction furnace," 2003, pp. 214–219.
17. D. Apelian and R. Mutharasan, "Filtration: A melt refining method," Journal of Metals, vol. 9, 1980, pp. 14-19.
18. B. Hübschen, J. Krüger, J. Keegan, and W. Schneider, "A new approach for the investigation of the fluid flow in ceramic foam filters," TMS Light Metals, 2000, pp. 809–815.
19. E. Moreira, M. Innocentini, and J. Coury, "Permeability of ceramic foams to compressible and incompressible flow," Journal of the European Ceramic Society, vol. 24, 2004, pp. 3209-3218.
20. F. Frisvold, "Filtration of aluminium: theory, mechanisms, and experiments," Norwegian University of Science and Technology, 1990.
21. S. Akbarnejad, R. Fritzsch, M. W. Kennedy, and R. E. Aune, "An Investigation on Permeability of Ceramic Foam Filters (CFF)," Accepted to 2015 TMS Annual Meeting & Exhibition, 2015.